Reduced clot debris size using standing waves formed via high intensity focused ultrasound

Shifang Guo,[1] Xuan Du,[1] Xin Wang,[1] Shukuan Lu,[1] Aiwei Shi,[1] Shanshan Xu,[1] Ayache Bouakaz,[1,2] and Mingxi Wan[1,a)]
[1]*The Key Laboratory of Biomedical Information Engineering of Ministry of Education, Department of Biomedical Engineering, School of Life Science and Technology, Xi'an Jiaotong University, Xi'an 710049, People's Republic of China*
[2]*Imagerie et Cerveau, Inserm UMR U930, Université François Rabelais, 37032 Tours, France*

(Received 3 July 2017; accepted 14 September 2017; published online 22 September 2017)

The feasibility of utilizing high intensity focused ultrasound (HIFU) to induce thrombolysis has been demonstrated previously. However, clinical concerns still remain related to the clot debris produced via fragmentation of the original clot potentially being too large and hence occluding downstream vessels, causing hazardous emboli. This study investigates the use of standing wave fields formed via HIFU to disintegrate the thrombus while achieving a reduced clot debris size *in vitro*. The results showed that the average diameter of the clot debris calculated by volume percentage was smaller in the standing wave mode than in the travelling wave mode at identical ultrasound thrombolysis settings. Furthermore, the inertial cavitation dose was shown to be lower in the standing wave mode, while the estimated cavitation bubble size distribution was similar in both modes. These results show that a reduction of the clot debris size with standing waves may be attributed to the particle trapping of the acoustic potential well which contributed to particle fragmentation. *Published by AIP Publishing*. [http://dx.doi.org/10.1063/1.4994038]

Thrombo-occlusive disease is a leading cause of mortality and morbidity worldwide.[1] Current clinical methods for the treatment of thrombosis include anticoagulant and thrombolytic drugs,[2–4] catheter-based endovascular techniques,[5,6] or a combination of both.[7] However, drugs without the use of a catheter are non-site-specific, require long treatment durations (several hours), and are associated with substantial risks of major bleeding. Catheter-based devices are used for localized treatments; however, an increased risk of bleeding is often observed, ultimately causing damages to the blood vessel walls and infection.[8] Furthermore, the applicability of this invasive procedure has recently been questioned due to the limited clinical feasibility compared to drug-alone treatments.[9]

Recent research studies have shown that ultrasound might be an effective thrombolytic method, as both a stand-alone procedure[10,11] and used in conjunction with thrombolytic drugs[12,13] or ultrasound contrast agents.[14,15] However, treatments that combine ultrasound with thrombolytic drugs may still cause drug-associated hemorrhage.[12] In addition, treatments in which ultrasound is used in combination with contrast agents may result in blood vessel damages due to the uncontrollable rupturing by ultrasound contrast agents.[16,17] Alternatively, the use of high intensity focused ultrasound (HIFU) to break up a blood clot has been reported both *in vitro*[10,18] and *in vivo*.[11,19,20] The overall benefits of this approach are as follows: localized treatments, clot lysis within minutes, and thrombolytic drugs are not required.

Although the feasibility of using HIFU to induce thrombolysis has been established, clinical concerns still remain regarding the produced clot debris via fragmentation of the original clot which may occlude downstream vessels due to their size, potentially causing hazardous emboli.[10,21] Therefore, it is essential to measure the size distribution of clot debris that results from HIFU-mediated lysis and explore methods designed to reduce the debris size. Current research on HIFU-induced thrombolysis has generally focused on the feasibility of using this technique to break clots.[11,22,23] However, only limited studies addressed the size distribution of clot debris.[10,21]

The vast majority of HIFU-mediated lysis is performed with travelling waves (TWs), commonly applied in medical diagnostics and therapies. So far, the impact of standing waves (SWs) on thrombolysis has not attracted much attention despite the fact that SWs offer several unique advantages over TWs, including a more spatially concentrated sound energy and a higher sound pressure in the focal region.[24] Even more importantly, the acoustic potential well generated by SWs may be used to manipulate particles,[25,26] potentially relevant to increase their interaction with HIFU waves and hence reduce the debris size in HIFU-induced thrombolysis. In this study, we investigate an approach for HIFU-based clot dissolution in which the SWs formed via HIFU are used to dissolve a thrombus and reduce the clot debris size. Additionally, the experiments were carried out at different flow velocities, considering the flow variation within body tissues.

A schematic representation of the experimental setup is shown in Fig. 1. A blood vessel phantom with a vessel diameter of 6 mm was placed in a water tank filled with degassed water and controlled using a 3-D position controller to ensure its proper location in the focal region of the ultrasound transducer. The signals generated from an arbitrary wave generator (AWG420, Tektronix, Beaverton, OR, USA) were amplified with a radio-frequency power amplifier (AG1017, T&G Power Conversion, Inc., Rochester, NY) and then sent to drive a 1.2 MHz concave HIFU transducer

a)Author to whom correspondence should be addressed: mxwan@mail.xjtu.edu.cn

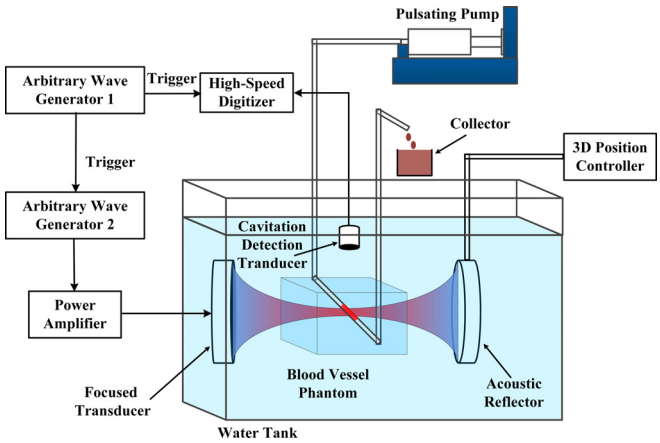

FIG. 1. Schematic representation of the experimental setup.

(Imasonic, Besancon, France) to transmit ultrasound with a peak negative pressure of 4.49 MPa at the focus for the TW mode. The active diameter and geometrical length of the transducer were 156 mm and 120 mm, respectively. An acoustic reflector (acoustical reflectivity R = 0.94) with the exact same shape as the HIFU transducer was placed centrosymmetrically around the focus to generate SWs as reported previously.[24] As a result, a SW field with basically the same outline as the TW field but with sharper rising and falling edges with a pitch of 0.6 mm (equal to the half-wavelength) was generated. Sound absorbers were attached on the walls of the tank to reduce reflected signals throughout the entire experiment. A 5 MHz single-element cavitation-detection transducer (bandwidth of 2.15–6.9 MHz, V309, Panametrics, Waltham, MA) was placed orthogonally to the axial direction of the HIFU transducer to receive the inertial cavitation signals. A high-speed digitizer (CS12400, Gage Applied, Inc. Lachine, QC, Canada) with a resolution of 40 ns was used to collect the received signals. Synchronization of the digitizer and the wave generator was achieved via an additional signal generator (Keysight Technologies, Inc., Santa Rosa, CA, USA). Saline solutions were pumped into the vessel with a pulsating pump (BT300-1F, Baoding Longer Precision Pump Co., Ltd., China). The pulse duration was 1 ms per pulse period (1/100 Hz = 10 ms), corresponding to a duty cycle of 10%. The treatment time for each trial lasted for 60 s. These parameters were similar to those used by other research groups[27] and ensured the generation of SWs. Preliminary experiments showed obvious thrombolysis using these transmitted parameters.

Fresh non-heparinized whole blood was collected from domestic rabbits and transferred into prepared glass tubes of identical size, through which a short segment of 4-0 silk suture had been threaded. The blood was allowed to coagulate at room temperature for 3 h and maintained at 4 °C for up to 3 days to allow for maximum clot retraction, lytic resistance, and stability.[28] Following this method, clots formed with high reproducibility in size (approximately 5 mm in diameter and 12 mm in height) and weight (170 ± 25 mg). All clots were carefully removed from the tubes and transferred to room-temperature saline (0.9% NaCl solution) for 2 h prior to the experiment and flushed with saline thrice to remove any fluids attached to the clots. The string with the attached thrombus was then carefully introduced into the phantom, and both the ends of the string were secured to hold the clot in the position under flow. The occlusion rate of the vessel was approximately 70%. Data were presented as mean ± standard deviation, and p-values were calculated using an independent t-test.

After each treatment, the solution containing suspended clot debris was collected in a clean, sterile beaker, and the size distribution of the debris particles was measured using a Coulter Counter particle sizing system (Multisize™ III, Beckman Coulter, USA). A 100 μm diameter aperture tube with a measurement range of 2–60 μm was used. As a result, debris larger than 60 μm or smaller than 2 μm could not be detected with this aperture tube. The sizing resolution was approximately 1% of the particle diameter. Two measurements were conducted for each sample. The number, mass, and size of the debris particles were used to summarize the debris particle size measurement. In the following equations, P_{ni} and P_{vi} represent the number and volume percentage of particles with diameters between D_{i-1} and D_i. D_i, P_{ni}, and P_{vi} represent the measurement outputs from the Coulter Counter. The average diameter D_{num}, calculated via the number percentage, and D_{vol}, calculated via volume percentage for each treatment, are defined as follows:

$$D_{num} = \sum_{D_i=2}^{D_i=60} P_{ni} \times D_i \tag{1}$$

$$D_{vol} = \sum_{D_i=2}^{D_i=60} P_{vi} \times D_i. \tag{2}$$

For each experiment, the emitted acoustic signals 10 s before treatment, 60 s during treatment, and 10 s after treatment were captured every second. The length of each capture was 30 ms which consisted of three bursts. Each signal was converted into the frequency domain to calculate the inertial cavitation dose (ICD) as described in Ref. 29. Furthermore, the diameter of the clot debris has been reported to be related to the cavitation bubble size distribution.[21] In this study, the size distribution of residual cavitation bubbles after different pulses was estimated using an acoustic method described in a paper previously published by our group,[30] which used a wide beam with low pressure to acquire the time intensity curve of the dissolution process for the bubbles with a combination of the bubble dissolution kinetics to determine the bubble size distribution. It should be noted that the estimation of the cavitation bubble size was performed in a separate experiment with the same acoustic parameters as those used in the investigation of clot debris, as wide beam detection of residual cavitation bubbles required several seconds and interrupted the clot lysis process.

Figure 2 shows the number and volume percentage of the clot debris particles in TWs and SWs at different flow velocities. Although the majority of the clot debris particles (more than 95% in number percentage) were below 10 μm in diameter [cf. Figs. 2(a)–2(c)], some large clot debris particles were also found to be generated, exhibiting a potential safety concern related to sonothrombolysis. The total number of produced particles after HIFU-thrombolysis exceeded ten

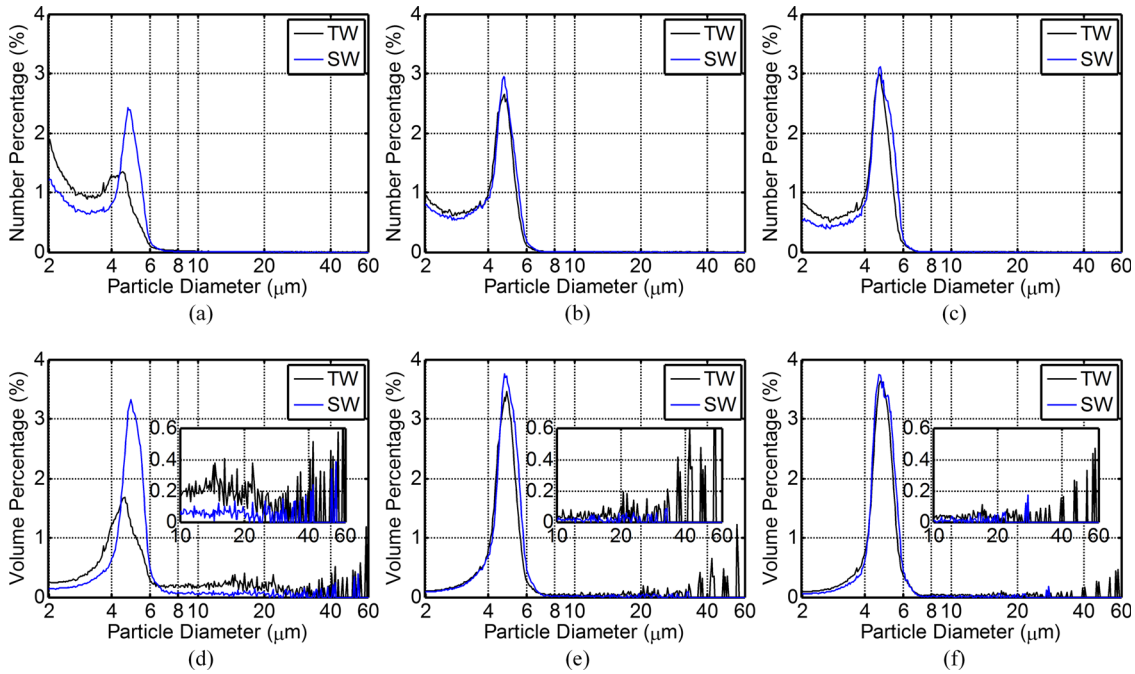

FIG. 2. Number and volume percentage of clot debris particles in TWs and SWs at different flow velocities. The velocities in (a) and (d) were 0 cm/s, (b) and (e) 4 cm/s, and (c) and (f) 10 cm/s, respectively. Repeat times n = 3. The inset pictures in (d)–(f) show a magnification view of the volume percentage of the particles between 10 μm and 60 μm.

millions (1.14×10^7 in TW and 1.33×10^7 in SW). This means that the total number of particles between 10 μm and 60 μm could be up to one hundred thousand. However, the mean diameter of the capillary was below 10 μm. Figures 2(d)–2(f) indicate that the volume percentage of large clot debris (larger than 10 μm) was lower in SWs than in TWs under identical thrombolysis conditions and considerably higher at low flow velocity. However, it is worth pointing out that the number percentage of debris between 2 μm and 4 μm decreased with the increasing flow velocity, particularly upon changing the flow velocity from 0 cm/s to 4 cm/s.

To quantify the changes of clot debris size distribution, the particles were organized in three groups as shown in Fig. 3: 2–10 μm, 10–30 μm, and 30–60 μm.[10,11] The results indicate that the volume percentage of small debris (2–10 μm) was lower in TWs than in SWs under static conditions, with a mean of 76.6% in the former and 88.4% in the latter. Furthermore, it was higher under flow conditions and significantly increased (p-value < 0.01) both in TWs (76.6% vs. 92.2%) and SWs (88.4% vs. 94.6%) when the flow velocity changed from 0 cm/s to 4 cm/s, respectively. However, for particle sizes ranging from 10 μm to 30 μm, it was clear that SW induced particle fragments were smaller than those produced in TWs. Under static conditions, the volume percentage of these particles decreased from 16.2% (4.7×10^4 in number) to 8.4% (2.6×10^4 in number) when SWs were used. The same trend could be observed for two other flow conditions, and a similar situation was observed for larger particles with sizes above 30 μm.

Figure 4 shows the average diameter of the clot debris calculated via number percentage and volume percentage at different flow velocities for both TW and SW modes. The results show that the average diameter calculated via number percentage remained approximately the same for both TW and SW modes and for all three flow velocities. However, the average diameter calculated via volume percentage was smaller in SWs than in TWs for all flow velocities. In addition, the average diameter decreased upon increasing the flow velocity. The reason for this contradiction was due to the number percentage of particles between 10 μm and

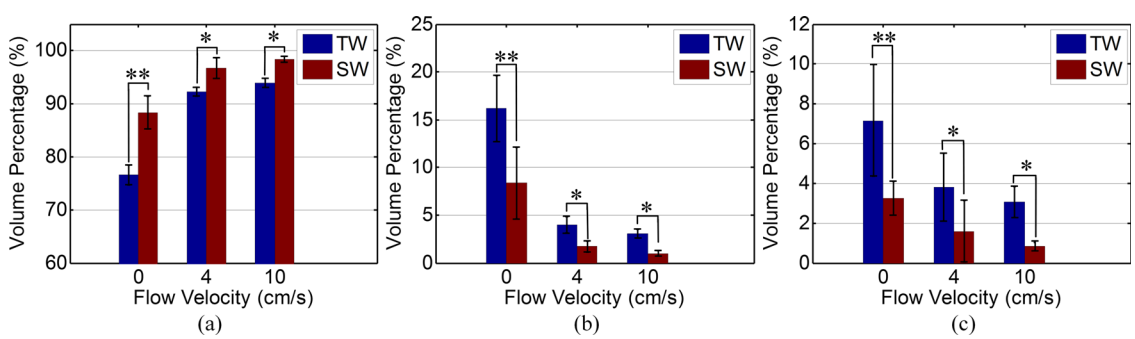

FIG. 3. Volume percentage of clot debris particles by the particle diameter between (a) 2 μm and 10 μm, (b) 10 μm and 30 μm, and (c) 30 μm and 60 μm, respectively, in TWs and SWs at different velocities (*$p < 0.05$ and **$p < 0.01$.).

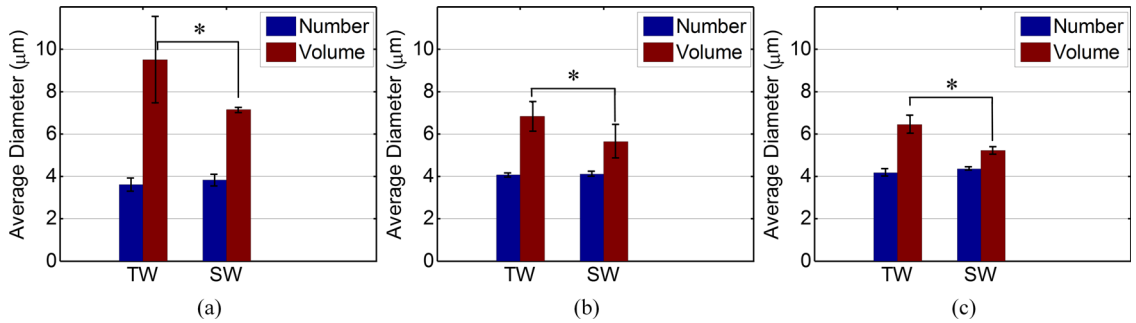

FIG. 4. Average diameter of the clot debris calculated via number percentage and volume percentage in TWs and SWs at different velocities. The velocities in (a)–(c) were 0 cm/s, 4 cm/s, and 10 cm/s, respectively. (*$p < 0.05$ and **$p < 0.01$.)

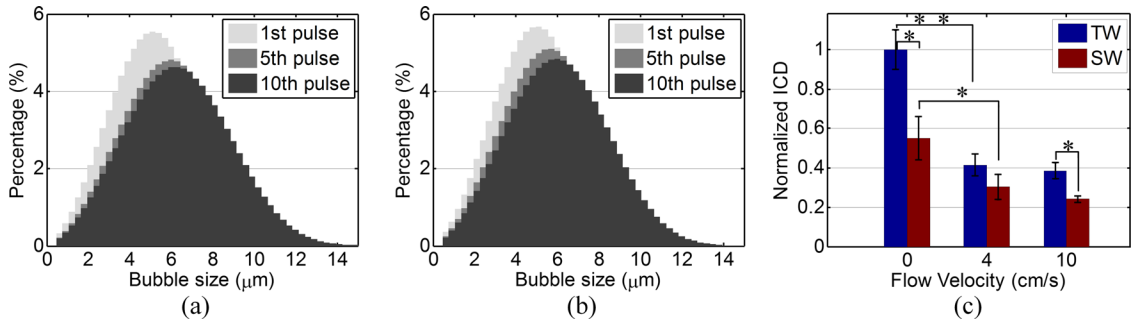

FIG. 5. Size distributions of the induced cavitation bubbles after the 1st, 5th, and 10th pulse in (a) TWs and (b) SWs under static conditions. (c) Normalized inertial cavitation dose generated during total treatment time at different flow velocities for two modes. (*$p < 0.05$ and **$p < 0.01$.)

60 μm that was below 5% resulting in a negligible influence on the average diameter calculated via number percentage. Taking into account that debris with a large size was more likely to occlude downstream vessels and cause hazardous emboli, the average diameter calculated by volume percentage of debris might be more suitable in the study of the thrombus fragment size distribution.

Figures 5(a) and 5(b) show that the size distribution of the cavitation bubbles from the 1st, 5th, and 10th pulse under static conditions increased slightly but exhibited a certain range after several pulses. The bubble distribution from multiple pulses was similar in both modes. Although it could not be estimated under the flow condition, the bubble size distribution under static conditions could be used as a reference. Figure 5(c) illustrates the variation of ICD at different velocities for two modes. The value of ICD was maximum under static conditions and was shown to be higher in TWs than that in SWs. Furthermore, the ICD value decreased rapidly upon increasing the flow velocity, particularly in the TW mode. Acoustic radiation force caused by the pressure gradient has already been shown to push debris and bubble clouds away from the focal region in the TW mode, thus limiting multiple effects of ultrasound on clot debris. Based on these results, a reduction of clot debris size was expected due to the following two parameters: First, the acoustic potential well generated in SWs could confine the clot debris to the focal region, further contributing to the fragmentation of clot debris. Second, blood flow may inhibit debris and bubble clouds to the upstream movement and push both into the focal area, resulting in a further debris fragmentation. It is worth pointing out in this context that a flow velocity that is too high may cause the debris to leave the focal region quickly, which may severely reduce the cavitation activity and further reduce the effectiveness of thrombolysis.

It is noteworthy that the peak negative pressure in SWs (7.36 MPa) was higher than that in TWs at fixed electrical power due to a more spatially concentrated sound energy at the focus, which was one of the unique advantages of using SWs. However, the clot debris size distributions and average diameters were demonstrated to exhibit no significant change (p-value > 0.05) in TWs when the pressure increased from 4.49 MPa to 7.36 MPa. Based on these results, it can be concluded that the reduced clot debris size in SWs may be attributed to the particle trapping of the acoustic potential well rather than a higher negative pressure.

In conclusion, this study demonstrates that a reduction of clot debris size can be achieved by using SWs formed via HIFU. The reduced ICD and similar cavitation bubble size in the SW mode indicated that the particle trapping of the acoustic potential well may be responsible for the reduction in size. Additionally, the debris size was smaller under flow compared to static conditions. Future work will further investigate the usefulness of this technique *in vivo* for the treatment of deep vein thrombosis in the calf of the leg.

This work was supported by Grants from the National Key Research and Development Program of China (No. 2016YFC0100701) and the National Natural Science Foundation of China (Grant Nos. 11474229 and 81471671).

[1]J. M. Escoffre and A. Bouakaz, *Therapeutic Ultrasound* (Springer, Berlin, 2015) p.339.
[2]S. Meairs, A. Alonso, and M. G. Hennerici, Stroke **43**, 1706 (2012).
[3]P. A. Kyrle and S. Eichinger, Lancet **365**, 1163 (2005).
[4]S. Moll, Arterioscler., Thromb., Vasc. Biol. **28**, 373 (2008).

[5]C. N. Gutt, T. Oniu, F. Wolkener, A. Mehrabi, S. Mistry, and M. W. Büchler, Am. J. Surg. **189**, 14 (2005).
[6]H. S. Kim, A. Patra, B. E. Paxton, J. Khan, and M. B. Streiff, Cardiovasc. Interventional Radiol. **29**, 1003 (2006).
[7]I. Alesh, F. Kayali, and P. D. Stein, Catheterization Cardiovasc. Interventions **70**, 145 (2007).
[8]S. Power, C. Matouk, L. K. Casaubon, F. L. Silver, T. Krings, D. J. Mikulis, and D. M. Mandell, Stroke **45**, 2330 (2014).
[9]A. Ciccone, L. Valvassori, M. Nichelatti, A. Sgoifo, M. Ponzio, R. Sterzi, and E. Boccardi, New Engl. J. Med. **368**, 904 (2013).
[10]A. D. Maxwell, C. A. Cain, A. P. Duryea, L. Yuan, H. S. Gurm, and Z. Xu, Ultrasound Med. Biol. **35**, 1982 (2009).
[11]C. Wright, K. Hynynen, and D. Goertz, Invest. Radiol. **47**, 217 (2012).
[12]M. Daffertshofer, A. Gass, P. Ringleb, M. Sitzer, U. Sliwka, T. Els, O. Sedlaczek, W. J. Koroshetz, and M. G. Hennerici, Stroke **36**, 1441 (2005).
[13]A. V. Alexandrov, C. A. Molina, J. C. Grotta, Z. Garami, S. R. Ford, J. Alvarez-Sabin, J. Montaner, M. Saqqur, A. M. Demchuk, L. A. Moyé, M. D. Hill, and A. W. Wojner, N. Engl. J. Med. **351**, 2170 (2004).
[14]S. Daniels, T. Kodama, and D. J. Price, Ultrasound Med. Biol. **21**, 105 (1995).
[15]D. Suo, Z. Jin, X. Jiang, P. A. Dayton, and Y. Jing, Appl. Phys. Lett. **110**, 023703 (2017).
[16]C. A. Molina, A. D. Barreto, G. Tsivgoulis, P. Sierzenski, M. D. Malkoff, M. Rubiera, N. Gonzales, R. Mikulik, G. Pate, J. Ostrem, W. Singleton, G. Manvelian, E. C. Unger, J. C. Grotta, P. D. Schellinger, and A. V. Alexandrov, Ann. Neurol. **66**, 28 (2009).
[17]N. J. McDannold, N. I. Vykhodtseva, and K. Hynynen, Radiology **241**, 95 (2006).
[18]X. Zhang, G. E. Owens, H. S. Gurm, Y. Ding, C. A. Cain, and Z. Xu, IEEE Trans. Ultrason. Ferroelectrics Freq. Control **62**, 1342 (2015).
[19]A. Burgess, Y. Huang, A. C. Waspe, M. Ganguly, D. E. Goertz, and K. Hynynen, PLoS One **7**, e42311 (2012).
[20]A. D. Maxwell, G. Owens, H. S. Gurm, K. Ives, D. D. Myers, Jr., and Z. Xu, J. Vasc. Interventional Radiol. **22**, 369 (2011).
[21]S. Xu, Y. Zong, Y. Feng, R. Liu, X. Liu, Y. Hu, S. Han, and M. Wan, Ultrason. Sonochem. **22**, 160 (2015).
[22]S. Westermark, H. Wiksell, H. Elmqvist, K. Hultenby, and H. Berglund, Clin. Sci. **97**, 67 (1999).
[23]V. Frenkel, J. Oberoi, M. J. Stone, M. Park, C. Deng, B. J. Wood, Z. Neeman, M. Hornelll, and K. C. P. Li, Radiology **239**, 86 (2006).
[24]H. Yin, Y. Qiao, H. Cao, Z. Li, and M. Wan, Ultrason. Sonochem. **21**, 559 (2014).
[25]A. Shi, Y. Min, and M. Wan, Appl. Phys. Lett. **103**, 174105 (2013).
[26]F. Petersson, A. Nilsson, C. Holm, H. Jönssonc, and T. Laurell, Lab Chip **5**, 20 (2005).
[27]C. Acconcia, B. Y. C. Leung, K. Hynynen, and D. E. Goertz, Appl. Phys. Lett. **103**, 053701 (2013).
[28]C. K. Holland, S. S. Vaidya, S. Datta, C. C. Coussios, and G. J. Shaw, Thromb. Res. **121**, 663 (2008).
[29]S. Zhang, Z. Cui, T. Xu, P. Liu, D. Li, S. Shang, R. Xua, Y. Zong, G. Niu, S. Wang, X. He, and M. Wan, Ultrason. Sonochem. **34**, 400 (2017).
[30]S. Xu, Y. Zong, W. Li, S. Zhang, and M. Wan, Ultrason. Sonochem. **21**, 975 (2014).